Population Estimation of Urban Residential Communities Using Remotely Sensed Morphologic Data

Yanhua Xie, Anthea Weng, and Qihao Weng, *Member, IEEE*

***Abstract*—Fine-scale population estimation in urban areas provides information useful in such fields as emergency response, epidemiological applications, and urban management. It is however a challenge because of lack of detailed building morphologic information. This research investigated the capability of LiDAR data for extraction of residential buildings and used the results for population estimation in heterogeneous environments in Indianapolis, USA. A morphological building detection algorithm was applied, to extract buildings from LiDAR point cloud, and yielded an overall detection accuracy of 95%. Extracted buildings were then categorized into nonresidential buildings, apartments, single-family houses, and other buildings based on selected geometric features (e.g., area, height, and volume) and background characteristics (vegetation and impervious cover) by a random forest classifier. Linear regression modeling, based on area, volume, and housing units, was applied to examine the relationship between census population and LiDAR-derived residential variables. The results show that morphological metrics extracted from LiDAR can be applied to classify buildings with relatively high accuracy, with an overall accuracy of 81.67%. The shape indexes contributed mostly to the residential building extraction followed by building background metrics. By excluding nonresidential buildings, the accuracy of population estimation increased from an RMSE of 20 and a mean absolute relative error (MARE) of 61.38% to an RMSE of 13 and a MARE of 33.52%. The differentiation between single-family houses and apartments contributed to the improved estimation. Additionally, the introduction of building height resulted in relatively accurate unit-based estimation. This study provides important insights into fine-scale population estimation in heterogeneous urban regions, when detailed building information is unavailable.**

***Index Terms*—Building classification, fine-scale population estimation, heterogeneous region, LiDAR, urban morphology.**

I. Introduction

POPULATION information in urban areas is significant for various demographic and socioeconomic applications. Although census data could provide broad-scale population information, collecting census information is usually time and labor intensive [1], [2]. The technologies of remote sensing and geographic information system provide a less expensive way to get population information. Remote sensing-derived variables (e.g., digital number, radiation value, or spectrally transformed variables) have been used as population indicators [3]. For previous studies, indicators were obtained from coarse- and moderate-spatial-resolution satellite imageries, such as nighttime light data, Moderate Resolution Imaging Spectroradiometer, and Landsat Thematic Mapper [4]–[6]. Simple models (e.g., linear model, exponential function, etc.) were applied to identify the relationship between population and the potential indicators [4], [6]. The main limitation for coarse- and moderate-resolution image-based methods is that the relationship between indicators and population is relatively weak, which makes these methods impossible for fine-scale population estimation. Building footprints and housing units extracted from high-spatial-resolution remotely sensed imagery (e.g., IKONOS and QuickBird) have shown to be more capable of providing more accurate fine-scale estimations [7]. While using high-spatial-resolution imagery in relatively homogeneous areas (e.g., suburban areas of a city) provided accurate estimations, the applications in heterogeneous urban regions (e.g., downtown area of a city), where a variety of building types (e.g., single-family house, apartment, and nonresidential buildings) may coexist, were unsatisfactory.

Volumetric approaches based on LiDAR-derived indicators have been proposed in area-based fine-scale population estimation [8]–[10]. For example, Upegui and Viel used a dasymetric method to estimate census block population with information from LiDAR-derived building volume for epidemiological applications [10]. However, the estimation accuracy was significantly impacted by the existence of nonresidential buildings (e.g., commercial buildings). In order to eliminate the influence of nonresidential buildings, Qiu *et al.* used parcel-based land use data to distinguish single-, two-, and multifamily buildings [8]. Similarly, Lu *et al.* utilized parcel data to categorize the usage of each building (e.g., single, multiple family, and nonresidential building) [9]. Their research suggested that building usage information was necessary for fine-scale population estimation in urban regions, particularly for heterogeneous sites. However, the usage information of urban buildings is not always available.

This study developed urban morphological metrics using LiDAR data and applied the metrics to fine-scale population estimation in Indianapolis, USA. Specifically, building types were categorized first based on selected shape features (including

Manuscript received October 23, 2014; revised November 26, 2014; accepted December 15, 2014.

Y. Xie and Q. Weng are with the Center for Urban and Environmental Change and the Department of Earth and Environmental Systems, Indiana State University, Terre Haute, IN 47809 USA (e-mail: qweng@indstate.edu).

A. Weng is with the Terre Haute South Vigo High School, Terre Haute, IN 47802 USA.

Color versions of one or more of the figures in this paper are available online at http://ieeexplore.ieee.org.

Digital Object Identifier 10.1109/LGRS.2014.2385597

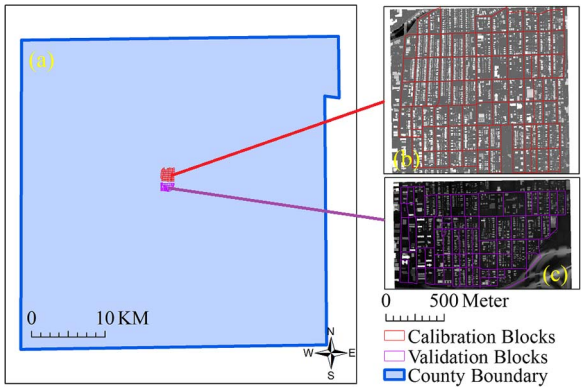

Fig. 1. Study area: (a) administrative boundary of Marion County, IN, USA; (b) calibration site; (c) validation site.

area, height, volume, compactness, etc.) and background characteristics (relationships between building, vegetation, and impervious surface). Population estimation at the census block level was then conducted based on the extracted residential building unit, area, and volume.

II. Study Area and Data Sets

Two sites located in the downtown area of Indianapolis, Indiana, USA, were selected as study areas (see Fig. 1). The landscape features in the areas include impervious surfaces (i.e., building, road, and parking area) and vegetation (i.e., grass and tree). Garages, single-family houses, multifamily buildings, apartments, nonresidential buildings (e.g., commercial buildings, churches, etc.) are mixed in the study areas. The complex landscape makes it challenging for fine-scale population estimation. The vegetation and roads are mainly distributed around residential buildings, while large parking lots are primarily located around nonresidential buildings.

Remotely sensed data, i.e., high-spatial-resolution orthophotography and LiDAR point cloud data, were acquired from the website of 2011 Indiana Statewide Imagery and LiDAR (http://gis.iu.edu/). The images have 0.15-m pixel resolution, and LiDAR data were produced at 1.0-m average post spacing with two collected return signals. The block boundary with 2010 census population was obtained from the United States Census Bureau. Building footprint file and property ownership data of 2012 were obtained from Indianapolis Mapping and Geographic Information Infrastructure (IMAGIS), City of Indianapolis, which detailed the extent and usage of each building and parcel. Orthophotography and property ownership data were used for calibration and validation of building classification, but they were supplemented by Google Street View and online parcel data (http://maps.indy.gov/MapIndy/), if necessary.

III. Methodology

Building footprints were first extracted from LiDAR data (i.e., first return height (FRH), last return height (LRH), bare surface height, and intensity surface). Building type categorization was then conducted using the random forest (RF) classifier and with morphological metrics extracted from LiDAR data. The area, volume, and housing unit were computed after building designation. Finally, the relationship between population and selected morphological variables was examined. Details of the research methodology are described in the following sections. The algorithms for building extraction, RF classifier, and model regression were implemented by using Matlab 2011b, and morphological metrics were calculated using the function of zonal statistics in ArcMap 10.1.

A. Building Extraction

LiDAR-derived surfaces were generated with 1.0-m pixel resolution. The modified morphological method proposed by Lu *et al.* was applied to delineate buildings [9]. The method included four steps: 1) threshold filtering, which filtered out nonbuilding pixels; 2) morphology filtering, which removed misclassified building pixels based on the morphological features of four neighboring pixels; 3) center recovering, which recovered incorrectly filtered pixels that were within buildings; 4) boundary recovering, which recovered misclassified building boundary pixels.

B. Building Type Classification Based on Morphological Metrics

1) RF Classifier: RF is a well-recognized classification and regression algorithm, which employs a set of expert trees (decision tree) to draw a conclusion by voting or averaging. One of the most appealing aspects of this algorithm is that it is reasonably accurate and not as sensitive to the configuration of training data sets as other classifiers, such as decision tree and support vector machine [11]. A detailed description about RF algorithm can be found in [12].

2) Extraction of Morphological Metrics: It has been demonstrated that shape features could help categorize buildings into residential/small buildings, apartments, and commercial buildings [13]. However, the confusion between apartments and commercial buildings implied that the introduction of merely shape indexes was not enough [13]. Thus, this study considered more morphological metrics, including: 1) basic statistics (BSI) of LiDAR-derived surfaces; 2) geometric features (GeF) of buildings; 3) landscape background information (BgI) of each building (see Table I).

To calculate the third group of the metrics, spatial and landscape attributes around buildings had to be obtained. In this letter, we classified background into three categories, i.e., grass, tree, and impervious surface (i.e., road/parking lot), based on the complexity of the landscape. Five hundred randomly distributed sample points were generated and then assigned to each group (i.e., grass, tree, and road/parking lot) by visual interpretation through the comparison between LiDAR intensity image, orthophotography, and Google Street View. Reference points located in buildings were detected by using extracted building footprints. Meanwhile, sample points that might have led to misassignation were deleted to enhance the quality of training data sets. The RF classifier was employed to classify building background based on intensity, FRH, LRH, first return slope (FRS), and last return slope (LRS).

3) Building Type Classification: Extracted buildings were linked to the property ownership data set to categorize them into

TABLE I
METRICS USED FOR BUILDING TYPE CLASSIFICATION

	Metrics	Description
BSI (1-6)	meanFRH	mean value of FRH for a building
	stdFRH	standard deviation of FRH for a building
	meanLRH	mean value of LRH for a building
	stdLRH	standard deviation of LRH for a building
	meanIn	mean intensity of a building
	stdIn	standard deviation of intensity of a building
GeF (7-15)	meanSlop	mean last return slope of a building's roof
	stdSlop	Standard deviation of LRS for a building roof
	meanH	mean height of a building
	stdH	standard deviation of height for a building
	Area	area of a building
	Perimeter	perimeter of a building
	Volume	volume of a building
	Cptness	compactness = 4*pi*Area/Perimeter
	SI	shape index = Perimeter/(4*sqrt(Area))
BgI (16-30)	NBDist	distance of the nearest building for a building
	blkBuildA	overall building area in a block
	blkBuildV	overall building volume in a block
	blkArea	area of a block
	numBuild	number of building in a block
	buildAR	specific building area/blkBuildA
	buildVR	specific building volume/blkBuildV
	impArea	area of impervious surface in a block
	grassArea	area of vegetation (i.e., grass) in a block
	treeArea	area of vegetation (i.e., tree) in a block
	treeVol	volume of vegetation (i.e., tree) in a block
	impR	ratio of impervious surface to blkArea
	buildR	ratio of building area to the area of a block
	grsR	ratio of grass area to the area of a block
	treeAR	ratio of tree area to the area of a block

garage, single-family building, apartment, or nonresidential building. Buildings with less than three units were assigned as single-family houses in this study, since they had similar morphologic characteristics. Half of the samples, which contained each building type, were used for model training, leaving the other half for validation. All trained decision trees were selected for building classification.

C. Population Estimation

The computation of building unit, area, and volume for each block was conducted after building classification. Nonresidential buildings were removed first, and then, the area and volume

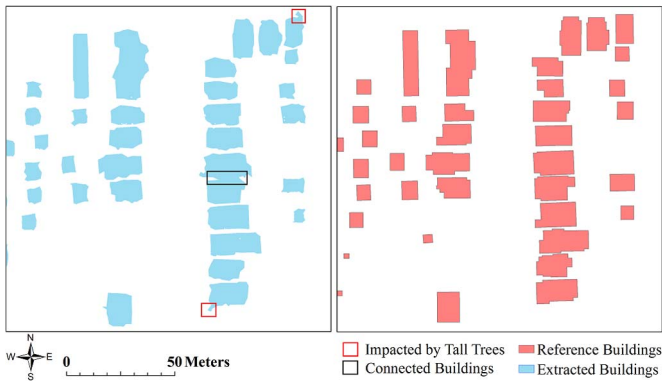

Fig. 2. Comparison between extracted and reference buildings.

of each residential building were calculated for each block. Residential building unit for a block referred to the unit number of single-family houses and apartments. The unit number of apartments was obtained by dividing the total volume of all apartments by the mean volume of a typical apartment building in the study area (approximately 388.83 m^3 in the study areas).

Linear regression modeling was performed to identify the relationship between LiDAR-derived variables and population at the block level. The independent variables were the unit/area/volume of the residential buildings in each census block. Next, we conducted multivariable regression modeling using the combination of these three variables. A detailed description of models can be found in [9]. The calibrated models were applied to estimate population for the validation site.

IV. RESULTS AND DISCUSSION

A. Building Extraction

The building footprint for the whole calibration site was extracted with an overall accuracy of 95.15% and a Kappa index of 0.85. Although the extraction accuracy was relatively high, there were still some limitations (see Fig. 2). For example, adjacent buildings tended to be linked together if they were too close to each other (closer than the LiDAR point spacing distance). Meanwhile, surrounding trees impacted the delineation of buildings, particularly for single-family residential houses. Thus, data-driven and model-driven methods may be combined to get more accurate building footprints in further researches [14].

B. Building Type Classification

A total of 133, 115, and 127 sample points for tree, grass, and road/parking, respectively, were finally collected. Fig. 3(a) and (b) shows randomly distributed training samples of impervious surface and vegetation, and the result of feature extraction, respectively. It shows that 50 trees might be enough to extract landscape features with accuracy of over 95%. Intensity played the most significant role on feature extraction, and without it, the overall accuracy may decrease by 30%. FRS was demonstrated as the second most important feature for landscape classification, followed by FRH and LRS.

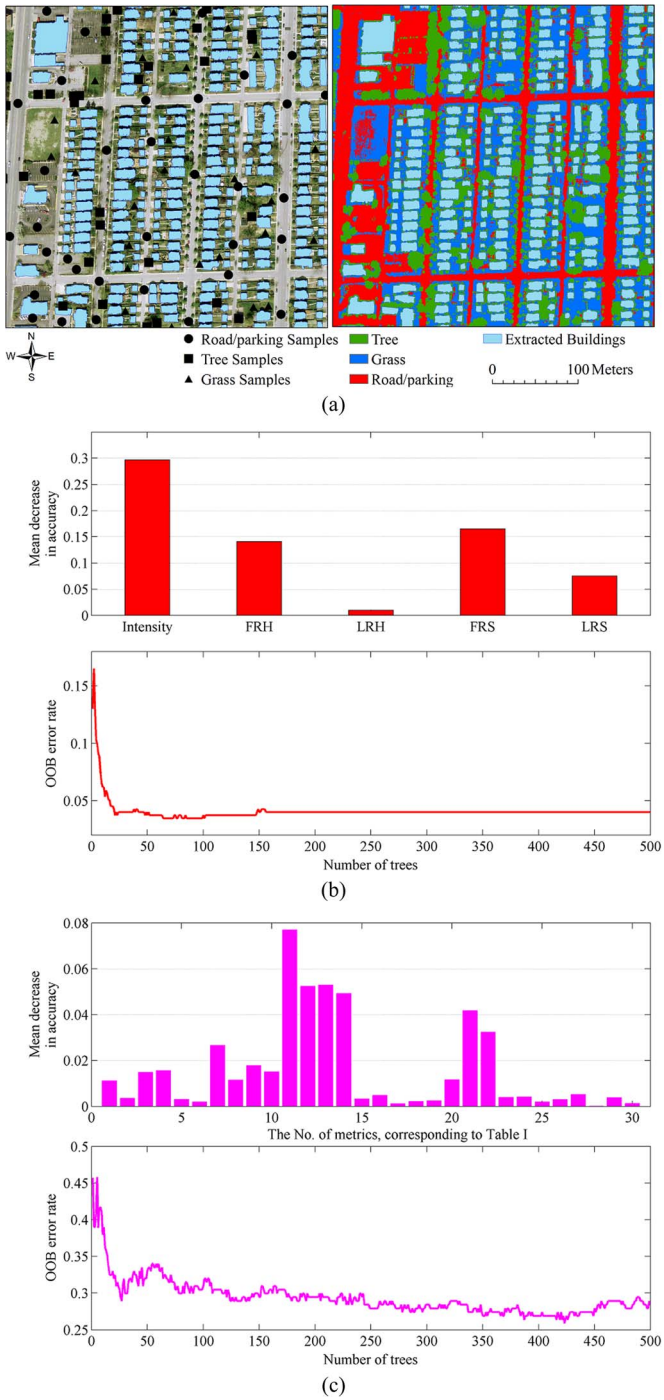

Fig. 3. (a) Distribution of training samples and the result of feature extraction for a part of the calibration site, (b) the importance of metrics and OOB error rate for feature extraction, and (c) the importance of features and OOB error rate for building extraction.

The numbers of nonresidential building, apartment, single-family house, and garage in the calibration site were 109, 68, 1187, and 640, respectively. To ensure the comparability between each group, only randomly selected 100 single-family houses and 100 garages were applied to test the effectiveness of the selected metrics for building classification. Fig. 3(c) indicates the importance and out-of-bag (OOB) error rate for classifier calibration. It is shown that 500 trees were enough to obtain a stable classification accuracy of around 70%. Shape indexes

TABLE II
ACCURACY ASSESSMENT OF BUILDING TYPE CLASSIFICATION BY USING RF CLASSIFIER

		Reference Building Type				User's Accuracy
		Non-res	*Apt*	*SF*	*Garage*	
Classified Building Type	Non-res	36	8	3	3	72%
	Apt	4	19	2	0	76%
	SF	6	3	45	0	83.33%
	Garage	4	0	0	47	92.16%
Producer's Accuracy		72%	63.33%	90%	94%	
Overall Accuracy		81.67%				
Kappa		0.75				

TABLE III
ACCURACY ASSESSMENTS FOR POPULATION ESTIMATION IN THE VALIDATION SITE

Model	R^2	RMSE[d]	MARE[e]	Model	R^2	RMSE[d]	MARE[e]
Area-based[a]	0.31	20	60.32%	Volume-based[b]	0.59	15	35.73%
Volume-based[a]	0.23	21	62.45%	Unit-based[c]	0.62	13	34.56%
Unit-based[b]	0.60	14	37.02%	Area-based[c]	0.68	13	28.27%
Area-based[b]	0.65	12	31.31%	Volume-based[c]	0.61	13	33.12%

[a] Regression using overall area or volume of buildings;
[b] Regression using only the unit/area/volume of residential buildings;
[c] Regression using multiple independent variables (i.e., the unit/area/volume ofsingle-family and apartment buildings, respectively);
[d] Root Mean Square Error; [e] Mean Absolute Relative Error.

(11)–(14) significantly contributed to building type classification, while buildAR and buildVR also played important roles. It is also found that the importance of intensity was negligible. A potential reason for this negligibility is that the buildings were constructed using similar materials, resulting in analogous intensity signals for LiDAR returns. Although building background metrics are useful to building type depiction, most of them contributed less than 1%. This may be because we used blocks to calculate the metrics.

Table II shows the accuracy of building classification. The overall accuracy was 81.67%, with a Kappa value of 0.75. Single-family buildings and garages were extracted with the producer's accuracy of 90% and 94%, and the user's accuracy of 83.33% and 92.16%, respectively. The accuracy of apartment extraction was the lowest, with the producer's and user's accuracy of 63.33% and 76%, respectively. A possible reason for this low accuracy was that apartments were often confused with nonresidential buildings due to their similar morphologic characteristics. The trained classifier was then applied to classify buildings in the validation site.

C. Population Estimation Using LiDAR-Derived Residential Variables

Table III lists the accuracy assessment of population estimation in the validation site for each model. The comparisons between models *a* and *b* or *c* show that, by conducting building classification, the accuracy of population estimation in the downtown area was dramatically improved. This is greatly attributed to the successful exclusion of nonresidential buildings, such as commercial buildings, churches, and garages. Another aspect is that the differentiation between single-family houses and apartments contributed to the improvement of population

estimation accuracy, although the contribution was not remarkable (i.e., comparisons between model b and c). This is due to the fact that residents that lived in apartments tended to possess less living space than those who dwelled in single-family buildings. Although the number of apartment units was incorrectly estimated due to the use of average volume of apartments, unit-based predictions yielded comparably reliable results compared to volume-based estimations. The solid outcome of unit-based estimations was attributed to the introduction of height information to the housing unit calculation. For a more accurate calculation of housing unit for population estimation, volume per apartment should be obtained with higher accuracy, instead of utilizing average volume. It is also worthy to note that volume-based models did not show significant superiority over area-based models. This might be the results of the relatively high ratio of single-family-dominated to apartment-dominated blocks and the number of single-family houses to that of apartments in most blocks.

There were some blocks with low population density, leading to significant overestimation for those blocks. In order to more accurately estimate population in those areas, other information, such as housing occupancy, should be utilized. Nighttime light data may be useful for the extraction of housing occupancy information. Current publicly available nighttime light data [e.g., imagery from Defense Meteorological Satellite Program's Operational Linescan System (DMSP/OLS) and Visible Infrared Imaging Radiometer Suite onboard NASA'S Suomi National Polar-orbiting Partnership (NPP/VIIRS)] is not so effective for fine-scale (block-level) population estimation. High-resolution nighttime images from the Earth Remote Observation Satellite-B (EROS-B) commercial satellite (spatial resolution $= 1$ m) might be useful [15]. The accuracy of population estimation in this study might have been influenced by the inconsistency of the data sets. For example, some residential buildings may be built or dismantled between the year 2010 and 2011. In addition, the accuracy of census population could also impact the model calibration. For instance, there were blocks with no residential buildings but residents.

V. Conclusion

Fine-scale population estimation in the urban areas is particularly difficult due to the unavailability of detailed residential building information. This research investigated the effectiveness of LiDAR data sets for the extraction of residential buildings for fine-scale population estimation in two urban areas of Indianapolis, USA.

The results showed that morphological metrics (i.e., shape indexes and building background metrics) extracted from LiDAR data could be successfully applied to classify buildings in the heterogeneous urban areas. Among the extracted features, shape features contributed the most to building type delineation. Meanwhile, the introduction of building background information improved the classification accuracy. Additionally, the separation of each building by usage significantly improved the accuracy of block-level population estimation. The differentiation between residential and nonresidential buildings and between single-family housing and apartment buildings contributed to a better population estimation.

However, limitations existed in both building type classification and population estimation. Building background metrics extracted from LiDAR data were block based, leading to the same background information for all buildings within the block. Thus, an alternative definition of building background metrics is needed. Meanwhile, housing occupancy information should be introduced for fine-scale population estimation, although it is not easy to obtain. In addition, block classification according to the characteristics of residential buildings (e.g., the proportion of single-family buildings) may enhance fine-scale population estimation, particularly for the estimation of population for a whole city.

References

[1] S. Ural, E. Hussain, and J. Shan, "Building population mapping with aerial imagery and GIS data," *Int. J. Appl. Earth Obs. Geoinf.*, vol. 13, no. 6, pp. 841–852, Dec. 2011.

[2] D. A. Swanson and G. C. Hough, "An evaluation of persons per household (PPH) estimates generated by the American Community Survey: A demographic perspective," *Popul. Res. Policy Rev.*, vol. 31, no. 2, pp. 235–266, Apr. 2012.

[3] C. Wu and A. T. Murray, "Population estimation using Landsat Enhanced Thematic Mapper imagery," *Geogr. Anal.*, vol. 39, no. 1, pp. 26–43, Jan. 2007.

[4] C. Lo, "Modeling the population of China using DMSP Operational Linescan System nighttime data," *Photogramm. Eng. Remote Sens.*, vol. 67, no. 9, pp. 1037–1047, 2001.

[5] J. E. Dobson, E. A. Bright, P. R. Coleman, R. C. Durfee, and B. A. Worley, "LandScan: A global population database for estimating populations at risk," *Photogramm. Eng. Remote Sens.*, vol. 66, no. 7, pp. 849–857, 2000.

[6] D. Lu, Q. Weng, and G. Li, "Residential population estimation using a remote sensing derived impervious surface approach," *Int. J. Remote Sens.*, vol. 27, no. 16, pp. 3553–3570, Aug. 2006.

[7] S. Wu, X. Qiu, and L. Wang, "Population estimation methods in GIS and remote sensing: A review," *GIsci. Remote Sens.*, vol. 42, no. 1, pp. 80–96, Mar. 2005.

[8] F. Qiu, H. Sridharan, and Y. Chun, "Spatial autoregressive model for population estimation at the census block level using LIDAR-derived building volume information," *Cartogr. Geogr. Inf. Sci.*, vol. 37, no. 3, pp. 239–257, Jan. 2010.

[9] Z. Lu, J. Im, and L. Quackenbush, "A volumetric approach to population estimation using LiDAR remote sensing," *Photogramm. Eng. Remote Sens.*, vol. 77, no. 11, pp. 1145–1156, Nov. 2011.

[10] E. Upegui and J.-F. Viel, "GeoEye imagery and lidar technology for small-area population estimation: An epidemiological viewpoint," *Photogramm. Eng. Remote Sensing*, vol. 78, no. 7, pp. 693–702, 2012.

[11] E. UPEGUI and J.-F. Viel, "Random forest: A classification and regression tool for compound classification and QSAR modeling," *J. Chem. Inf. Comput. Sci.*, vol. 43, no. 6, pp. 1947–1958, 2003.

[12] L. Breiman, "Random forests," *Mach. Learn.*, vol. 45, no. 1, pp. 5–32, Oct. 2001.

[13] M. Belgiu, I. Tomljenovic, T. J. Lampoltshammer, T. Blaschke, and B. Höfle, "Ontology-based classification of building types detected from airborne laser scanning data," *Remote Sens.*, vol. 6, no. 2, pp. 1347–1366, Feb. 2014.

[14] A. Henn, G. Gröger, V. Stroh, and L. Plümer, "Model driven reconstruction of roofs from sparse LIDAR point clouds," *ISPRS J. Photogramm. Remote Sens.*, vol. 76, pp. 17–29, Feb. 2013.

[15] N. Levin, K. Johansen, J. M. Hacker, and S. Phinn, "A new source for high spatial resolution night time images—The EROS-B commercial satellite," *Remote Sens. Environ.*, vol. 149, pp. 1–12, Jun. 2014.